ELSEVIER

Polymer 44 (2003) 2411–2422

polymer

www.elsevier.com/locate/polymer

Reactive compatibilizer precursors for LDPE/PA6 blends. II: maleic anhydride grafted polyethylenes

Cuihong Jiang[a,1], Sara Filippi[b], Pierluigi Magagnini[b,*]

[a]*Department of Chemistry, Rutgers University, Newark, NJ, USA*
[b]*Dipartimento di Ingegneria Chimica, Chimica Industriale e Scienza dei Materiali, Università degli Studi di Pisa, via Diotisalvi 2, 56126 Pisa, Italy*

Received 7 October 2002; received in revised form 15 January 2003; accepted 3 February 2003

Abstract

Several home made and commercially available polyethylene (PE) samples grafted with maleic anhydride (MA) (PE-*g*-MA) were used as compatibilizer precursors (CPs) for the reactive blending of low density PE (LDPE) with polyamide-6 (PA). Scope of the work was to compare the effectiveness of these CPs with that of a number of ethylene–acrylic acid copolymers (EAA), which had been employed in a previous study for the reactive compatibilization of the same blends, and to get a deeper insight into the coupling reactions producing the PA-*g*-CP copolymers that are thought to act as the true compatibilizers in these systems. To this end, binary CP/LDPE and CP/PA and ternary LDPE/PA/CP blends were prepared with a Brabender mixer and were characterized by DSC, SEM and solvent fractionation. The results show that the PE-*g*-MA copolymers react more rapidly with PA than the EAA copolymers and that their CP effectiveness depends critically on the microstructure and the molar mass of their PE backbones. In particular, the CPs produced by functionalization of LDPE were shown to be miscible with this blend component and to be scarcely available at the interface where reaction with PA is expected to occur. Conversely, the CPs prepared from the HDPE grades were immiscible with LDPE and showed better CP performance. Whereas the effectiveness of the EAA copolymers studied earlier had been shown to increase with an increase in the concentration of the carboxyl groups, the concentration of the succinic anhydride groups of the PE-*g*-MA CPs studied in this work was found to play a minor role, at least in the investigated range (0.3–3.0 wt% MA).

Keywords: LDPE/PA blends; PE-*g*-MA compatibilizer precursors; Morphology

1. Introduction

Blends of polyethylene (PE) with polyamide-6 (PA) may lead to polymers possessing a synergic combination of the typical properties of PE, namely, low cost, processability, resilience and moisture insensitivity, with those of PA, i.e. rigidity, thermal stability and barrier properties to oxygen and solvents, provided that the blends are appropriately compatibilized [1,2].

Block or graft copolymers formed in situ by reaction of the blend components with compatibilizer precursors (CPs) consisting of polyolefins containing succinic anhydride functional groups, have been extensively investigated as compatibilizers for PE/PA blends [3–20]. Numerous studies have demonstrated that the addition of CPs functionalized with maleic anhydride (MA) into the PE/PA blends greatly improves the blends properties by strongly enhancing the dispersion of the minor phase droplets, hindering (or suppressing) their coalescence, and improving interfacial adhesion. Also, they have shown that the effectiveness of the CPs depends not only on their chemical composition, but also on the relative molar mass of all the components and on the blending conditions. Thus, the influence of the concentration and the molecular weight of maleated CPs on the morphology and the properties of blends of PA with a mixture of HDPE and LLDPE has been studied by Padwa et al. [5]. Kudva et al. [15] described the effect of the concentration and the functionality of a series of LLDPE-*g*-MA copolymers, as well as the influence of the molar mass of the components, on the rheological, morphological and mechanical properties of binary PA/CP blends and of ternary LLDPE/PA/CP blends. Jurkovski and

* Corresponding author. Tel.: +39-050-511222; fax: +39-050-511266.
E-mail address: magagnini@ingunipi.it (P. Magagnini).
[1] Present address: Laboratory of Surface Science and Technology, University of Maine, Orono, ME 04468, USA.

0032-3861/03/$ - see front matter © 2003 Elsevier Science Ltd. All rights reserved.
doi:10.1016/S0032-3861(03)00133-2

coworkers [10,17,20] investigated the influence of the blending conditions on the mechanochemical compatibilization of PA/LDPE blends carried out in the presence of a LDPE-*g*-MA copolymer. Pan et al. [18,19] studied the shear induced pullout, from the interface, of graft copolymers formed in situ by reaction of PA with maleic anhydride- or glycidylmethacrylate-functionalized PE samples, and discussed the effect of the length of the PA and PE branches. However, a direct comparison between these experiments, which involved different grades of PE, blending conditions, and CPs structures, is not easy. Similarly, it is difficult to determine from these studies the relative efficiency of CPs containing different reactive groups.

The first paper of this series [21] described the use of ethylene-acrylic acid copolymers (EAA) with different AA contents as CPs for blends of two grades of LDPE with PA, in the whole composition range. In that work we have shown that the addition of only 2 phr of these CPs into the LDPE/PA blends improves the interfacial adhesion, enhances the minor phase dispersion and hinders the droplets coalescence. The carboxyl groups of the CPs react with the amine and/or amide groups of PA to form CP-*g*-PA copolymers and the effectiveness of the different CPs increases with a decrease in their molar mass and with an increase of the concentration of acrylic acid moieties. In this work we compare the effectiveness of PE-*g*-MA copolymers with that of the EAA copolymers studied previously, in view of the reactive compatibilization of the same LDPE/PA blends. In this set of experiments, we used two grades of HDPE-*g*-MA copolymers, one commercially available and one home made, having different molar mass, and several purposely prepared LDPE-*g*-MA copolymers with different MA content (0.3–3.0 wt%). The results of the morphological, thermal and rheological characterization of both binary and ternary blends were compared with those of the previous study [21].

2. Experimental

2.1. Materials

Two grades of LDPE, kindly provided by Polimeri Europa, were used: Riblene FF20 with MFI = 0.8 g/10 min and $d = 921$ kg/m^3, referred to herein as LD08, and Riblene FC30 (LD03) with MFI = 0.27 g/10 min and $d = 922$ kg/m^3. The polyamide-6 (PA) sample was kindly supplied by Snia Tecnopolimeri; its relative viscosity in sulfuric acid (95.7%) was 3.66 and the contents of amine and carboxyl end groups were 34 and 35 mequiv./kg, respectively. LD08 and a commercial sample of HDPE, referred to as h-HDPE, with MFI = 1.76 g/10 min, by Solvay, were used for the synthesis of the LDPE-*g*-MA and h-HDPE-*g*-MA compatibilizer precursors. A commercial MA functionalized HDPE sample of lower molar mass (Polybond 3009, with MFI = 5.0 g/10 min and 1.0 wt% MA), indicated as l-HDPE-*g*-MA, was kindly provided by Uniroyal. Before use, all the polymers were accurately dried under vacuum for 12 h at 70 °C (for the PE and PE-*g*-MA samples) or 120 °C (for PA). Maleic anhydride (95% purity, by Aldrich), styrene (by Aldrich), and dicumyl peroxide (by AtoChem) were used as received.

2.2. Polyethylene functionalization

LD08-*g*-MA, with 0.3–3.0 wt% MA, and h-HDPE-*g*-MA, with 1.1 wt% MA, were synthesized by melt free radical grafting, according to procedures described in the literature [22,23]. The polyolefins were blended with MA in a Brabender Plasticorder internal mixer of 50 ml capacity at 150 °C for LD08, and 170 °C for h-HDPE, with a rotor speed of 70 rpm, under nitrogen flux. Dicumyl peroxide (DCP) was used as an initiator, and styrene was employed as a comonomer to prevent crosslinking. In a typical melt-grafting reaction, the calculated amounts of powdered PE, MA and DCP were premixed, charged into the preheated mixer and blended for 8 minutes. The functionalized PE was purified by dissolving about 5.0 g of the crude product in 200 ml of boiling xylene and pouring the hot solution into excess acetone, with vigorous stirring. The content of grafted succinic anhydride groups was determined by titration with known procedures [24–26]. About 1.0 g purified product was dissolved in 100 ml xylene, and the solution was refluxed for 40 min; successively, 3 ml water was added to hydrolyze the anhydride groups; after 25 min, the hot solution was added with excess KOH solution in ethanol (0.025N) and back titrated with HCl in ethanol (0.025N), with phenolphthalein as an indicator. The PE-*g*-MA samples were also characterized by FTIR spectroscopy [22–24]. The spectra were obtained using thin films prepared on a laboratory press at 200 °C and 2 MPa. The ratio of the intensities of the peaks at 1858 cm^{-1}, characteristic of the five-membered cyclic anhydride carbonyls, and at 720 cm^{-1}, due to the rocking vibration of the methylene sequences, was used together with the results of the titrations to get a calibration curve.

2.3. Blends preparation

The appropriate amounts of all the components, previously dried as described above, were dry-blended and introduced in the 50 ml mixing bowl of a Brabender Plasticorder preheated to 235 °C. The rotor speed was held at 30 rpm during loading and was then increased to 60 rpm. Blending was continued for 4 min. During this period, temperature and applied torque were continuously recorded. At the end, the molten blends were rapidly quenched in icewater.

2.4. Molau test

In order to qualitatively prove that PA-*g*-CP copolymers

did actually form during the blending of PA with the PE-*g*-MA samples, the Molau test [27,28] was carried out by stirring about 2 g of the powdered binary blends in 50 ml of 85% formic acid for 2 h. The test tubes were then stored for 24 h and the formation of a stable suspension or of a turbid colloidal solution was taken as an indication of the presence of a PA-*g*-CP copolymer acting as a surfactant.

Quantitative solvent fractionation experiments were also carried out on the binary blends, using formic acid and hot xylene as selective solvents, and the soluble and insoluble fractions were separated by centrifugation of the suspensions and characterized.

2.5. Morphological analysis

Scanning electron microscopy (SEM) observations of cryofractured blends samples coated with gold were made with Jeol JSM-5600LV or Jeol T300 microscopes. Analysis of the size and size distribution of the minor phase droplets was done on micrographs taken on solvent etched fracture surfaces with an automatic image software. Two or more micrographs of each sample were analyzed for a total of at least 500 particles. The number average diameter (d_n) was calculated from the relationship [29] $d_n = \sum(n_i d_i)/\sum n_i$, where n_i is the number and d_i is the diameter of the ith droplet. The frequency plots were drawn by counting the particles with a size step of 0.10 μm and fitting the data with Gaussian curves.

2.6. Thermal analysis

Differential scanning calorimetry (DSC) measurements were carried out under nitrogen, on samples of 5–8 mg, using a Pyris Perkin–Elmer apparatus. The pure polymers were pretreated in the Brabender mixer under the same conditions used for blending. The scanning rate was of 10 K/min. The first heating scan was carried out from 20 to 250 °C and the sample was held at this temperature for three minutes, to cancel the thermal history effects, before starting the cooling and the second heating sweeps, which were used for Figures and Tables. The temperature ranges used for measuring the ΔH values were normally as follows: 70–110 °C (cooling) and 75–125 °C (heating) for the LDPE and LDPE-*g*-MA phases; 80–125 °C (cooling) and 90–145 °C (heating) for the HDPE and HDPE-*g*-MA phases; 170–195 °C (cooling) and 185–235 °C (heating) for the PA phase. The values of ΔH were usually normalized to the amount of the phase under consideration in order to get information on its degree of crystallinity. ΔH values normalized to the overall amount of the sample were used, e.g. in Table 3, whenever the exact concentration of the relevant component was unknown and was just approximately calculated from the ΔH values.

3. Results and discussion

The synthesis of LD08-*g*-MA and h-HDPE-*g*-MA occurred easily, with a yield of grafted MA of 25–50% and negligible crosslinking, when approximately equivalent amounts of MA and styrene comonomer (1–10 phr) and 0.1–0.5 phr DCP were used. Several LD08-*g*-MA copolymers with an MA content ranging between 0.3 and 3.0 wt% and one h-HDPE-*g*-MA sample with 1.1 wt% MA were prepared.

The thermal properties of all the CPs used for the blends preparation are listed in Table 1, together with those of the neat polymers. It may be observed that the transition temperatures of LD08 are almost unaffected by grafting, whereas the associated enthalpies become slightly smaller as the content of grafted MA increases.

3.1. Binary CP/PE and CP/PA blends

The thermal characteristics of some of the binary CP/PE and CP/PA blends studied in this work are presented in Table 2. For the LD08-*g*-MA/LD08 blends, the thermal properties were substantially independent of the MA content of the CP: for this reason, only the data for the blend with LD08-*g*-MA (3.0 wt%) are reported in the Table. The DSC traces of these blends were practically carbon copies of those of LD08, and this is why they were not shown in Fig. 1. This coincidence is most probably due to miscibility of the two polymers; however, such conclusion cannot be definitely drawn on the basis of the thermal data only, because simple superposition of the transitions of LD08-*g*-MA and LD08 might also produce the observed results. The DSC traces of the blends of the two HDPE-*g*-MA CPs with LD08, shown in Fig. 1, on the contrary, demonstrate clearly that these materials are biphasic. The two phases are highly compatible, however, as demonstrated by the broadening of the transition peaks of the LD08 phase and the reduction of T_m and T_c of the CP phases.

The micrographs in Fig. 2 illustrate the morphology of the binary CP/LD08 blends. Practically complete homogeneity can be observed for the 20/80 LD08-*g*-MA/LD08 blend (Fig. 2a), whereas two phases, though highly adherent, are

Table 1
Thermal properties of the blends components

Material	T_c (°C)	ΔH_c (J/g)	T_m (°C)	ΔH_m (J/g)
LD08	96.6	82.3	110.9	84.0
LD03	97.6	80.3	110.4	87.4
PA	187.6	69.8	219.4	67.7
LD08-*g*-MA (0.3 wt%)	96.6	79.0	111.0	81.9
LD08-*g*-MA (0.8 wt%)	96.5	76.9	111.0	81.5
LD08-*g*-MA (1.8 wt%)	96.6	74.8	111.3	80.3
LD08-*g*-MA (2.4 wt%)	96.6	73.6	111.2	78.2
LD08-*g*-MA (3.0 wt%)	96.3	69.0	109.2	76.5
h-HDPE-*g*-MA (1.1 wt%)	115.1	150.9	132.4	169.3
l-HDPE-*g*-MA (1.0 wt%)	112.1	152.9	129.5	175.1

Table 2
Thermal properties of the binary 20/80 CP/PE and CP/PA blends

Blend	CP phase				LD08 or PA6 phase			
	T_c (°C)	ΔH_c [a] (J/g)	T_m (°C)	ΔH_m [a] (J/g)	T_c (°C)	ΔH_c [a] (J/g)	T_m (°C)	ΔH_m [a] (J/g)
LD08-MA (3.0 wt%) /LD08	–	–	–	–	96.4	78.2[b]	110.1	79.8[b]
h-HDPE-*g*-MA/LD08	115.6	113.3	126.6	126.6	97.3	91.1	109.4	109.6
l-HDPE-*g*-MA/LD08	108.3	139.2	121.3	131.7	98.9	80.3	107.9	104.1
LD08-*g*-MA (3.0 wt%)/PA	95.7	72.3	108.4	55.6	185.2	53.9	218.5	56.0
h-HDPE-*g*-MA/PA	115.1	156.7	128.5	148.8	186.8	54.8	215.5	53.1
l-HDPE-*g*-MA/PA	102.7	138.4	124.4	136.7	185.1	52.2	217.6	53.9

[a] Values normalized to the amount of the relevant phase.
[b] Values normalized to the total amount of the blend.

clearly visible for the HDPE-*g*-MA/LD08 blends (Figs. 2b and c). These results are in agreement with those of the DSC characterization.

The thermal properties of the binary CP/PA blends collected in Table 2 are indicative of interactions between the phases that seem particularly noticeable for the blend with l-HDPE-*g*-MA. In fact, the temperatures and the enthalpies associated with the transitions of both phases of this blend are lowered with respect to those of the pure polymers given in Table 1. Moreover, as it is shown in Fig. 3, blending of PA with the CPs leads to changes in the shape of the melting peak of the PA phase: in particular, for the blend with l-HDPE-*g*-MA, the intensity of the lower temperature melting peak, corresponding to the γ phase crystals, is considerably increased.

The SEM micrographs of the 20/80 CP/PA blends, before and after etching with boiling xylene, are shown in Fig. 4. They show that the dispersion of the minor phase

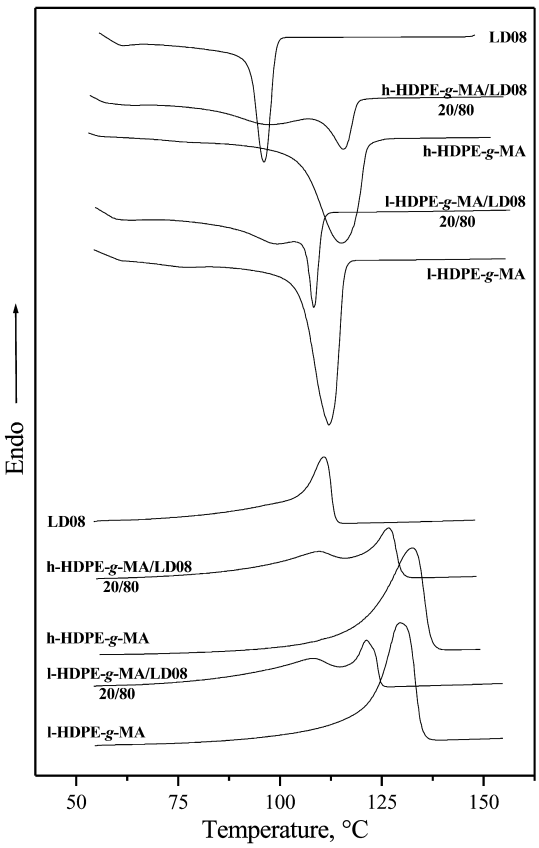

Fig. 1. DSC traces of the 20/80 HDPE-*g*-MA/LD08 blends and of their components.

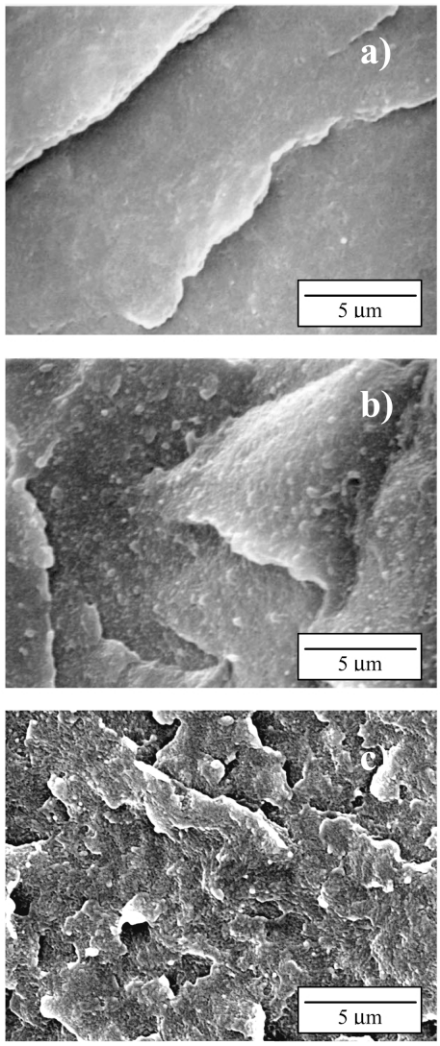

Fig. 2. SEM micrographs of the 20/80 CP/LD08 blends; (a) CP = LD08-*g*-MA (3.0 wt%); (b) CP = h-HDPE-*g*-MA; (c) CP = l-HDPE-*g*-MA.

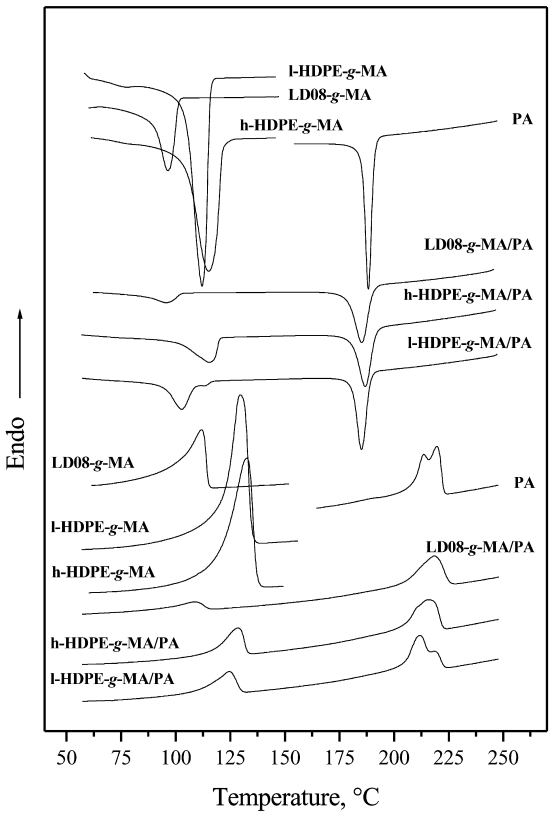

Fig. 3. DSC traces of the 20/80 CP/PA blends and of their components.

droplets is very fine, and that there is good interfacial adhesion between the phases. A comparison of the micrographs seems to confirm the conclusion of the DSC analysis, i.e. that the interactions of PA with l-HDPE-*g*-MA are probably stronger than those with the other CPs.

As illustrated in Scheme 1, the CP-*g*-PA copolymers may form by reaction of the succinic anhydride groups of the CPs either with the amine end groups of PA, or with the in-chain amide groups. According to the first mechanism, the formation of the imide bond linking the PA graft to the CP chain involves the evolution of a water molecule. In the blending conditions, the water may promote the hydrolysis of PA, so that the two reaction mechanisms do in fact lead to the same products. According to the results of model experiments carried out by Maréchal et al. [30], the reactions involved in mechanism (a) are considerably faster than that of mechanism (b), despite the much higher concentration of the amide groups with respect to the amine end groups.

Solvent fractionation experiments were performed to investigate the composition of the binary CP/PA blends listed in Table 2. Room temperature treatment of small blends samples with 85% formic acid, a solvent of the matrix PA phase, yielded fine suspensions that were still turbid after 24 h. When the same procedure was employed with 25/75 HDPE/PA and LD08/PA blends, we observed a clean separation of the insoluble PE phase from the clear PA solution. This qualitative test, referred to as the Molau test [27,28] is routinely used [6,8,9,12,21,31,32] to demonstrate the presence of block or graft polyolefin/PA copolymers that, acting as surfactants, stabilize a colloidal suspension of polyolefin particles in the PA solution.

The fractionation was carried out as shown in Scheme 2. The suspensions in formic acid were centrifuged to separate an insoluble residue, referred to as R^1_{insol}, from a turbid solution. The solution was poured into excess ethanol to precipitate the formic acid soluble fraction, R^1_{sol}. The insoluble fraction R^1_{insol} was treated with boiling xylene (a good solvent for the CPs) and the resulting hot suspension was centrifuged to separate the insoluble material, R^2_{insol}, from a clear solution that yielded the xylene soluble material (R^2_{sol}) by precipitation into methanol. The R^2_{insol} fractions were extracted again with formic acid with negligible weight loss.

The yields and the thermal properties of the four fractions of each of the three 20/80 CP/PA blends are given in Table 3. As mentioned in the previous section, the R^1_{sol} fraction was obtained by pouring the formic acid solution into excess ethanol. Even after centrifugation, the formic acid solution was slightly opalescent, for the blends with LD08-*g*-MA and h-HDPE-*g*-MA, and turbid for the blend with l-HDPE-*g*-MA. From the DSC traces of the three R^1_{sol} fractions, the presence of a measurable amount of CP could only be recorded for the latter blend. Obviously, this does not exclude that CP sequences may be present also in the R^1_{sol} fractions of the other two blends, either as suspended colloidal particles and as short segments of dissolved CP-*g*-PA copolymers. Despite the possible presence of some CP-*g*-PA in the formic acid soluble fractions, their amount (as an average, about 70% of the overall mass of the blends) was always less than the initial PA content (80%). This means that some PA remained in the formic acid insoluble fraction R^1_{insol}, presumably as a CP-*g*-PA copolymer.

Similar formic acid extraction experiments carried out in the previous work [21] on the binary blends of EAA copolymers with PA led to quite different results. While the formation of CP-*g*-PA copolymers was clearly demonstrated also for the EAA/PA blends, the amount of soluble material was always found to exceed the initial content of PA, indicating that a considerable part of these copolymers could not be separated as an insoluble material. These differences can be explained if one considers that the number of free carboxyl groups in the EAA copolymers (containing 6–11 wt% acrylic acid, or 0.82–1.51 mol/kg) is considerably higher than that of the succinic anhydride moieties of the CPs employed in this work (0.3–3.0 wt%, or 0.03–0.31 mol/kg). Therefore, the average number of PA branches in the EAA-*g*-PA copolymers was probably larger, and the solubility in formic acid higher.

In order to determine the composition of the different fractions listed in Table 3, one could obviously use the ΔH_c and ΔH_m values measured by calorimetry for the first order transitions of the two phases. However, their degree of crystallinity was unknown and, therefore, just a rough

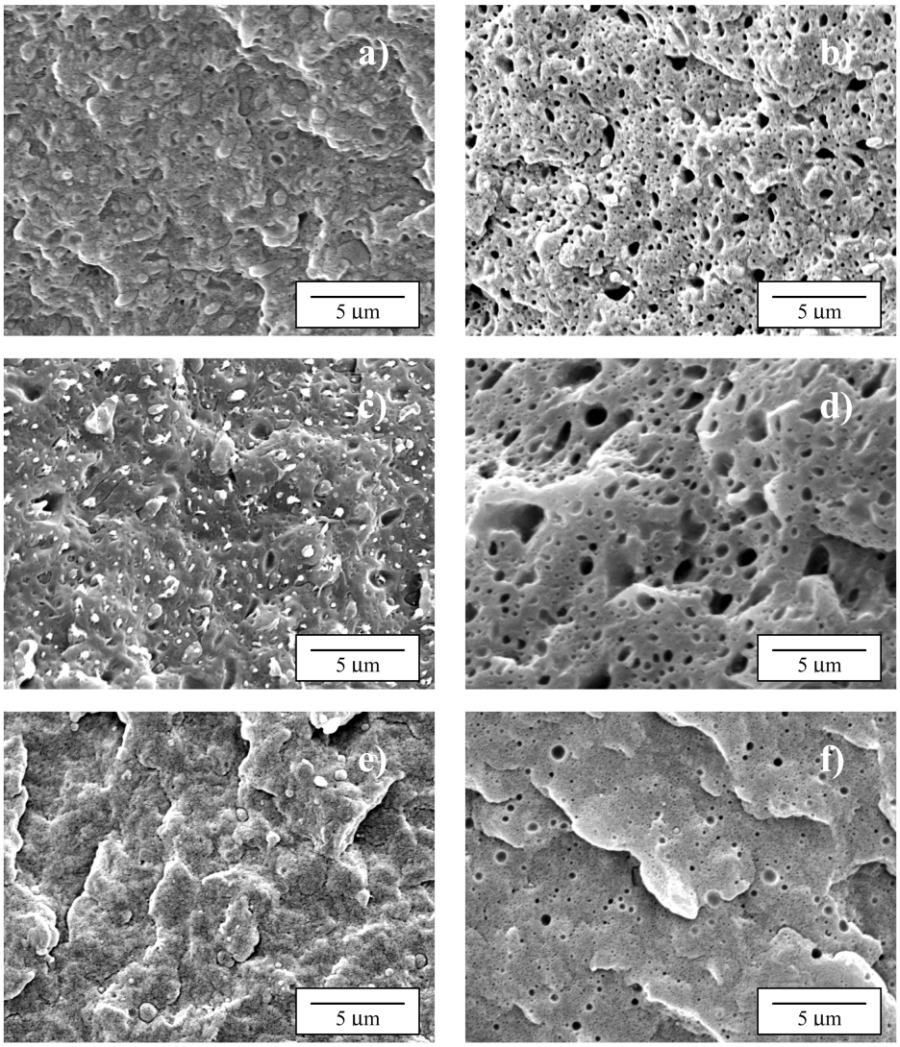

Fig. 4. SEM micrographs of the 20/80 CP/PA blends, before (a, c, e) and after (b, d, f) etching with boiling xylene. (a, b) CP = LD08-*g*-MA (3.0 wt%); (c, d) CP = h-HDPE-*g*-MA; (e, f) CP = l-HDPE-*g*-MA.

estimation of the composition of the fractions could be made by comparing their DSC traces with those of the pure components, given in Table 1, and of the binary blends of known composition, reported in Table 2. The obtained values were then corrected considering that the sum of the contents of, e.g. CP in R^1_{sol} and R^1_{insol}, multiplied by the yields of these fractions, should be equal to the CP content in the original blend, and that the concentration of CP in the R^1_{insol} fraction should be equal to the sum of the contents of the same component in R^2_{sol} and R^2_{insol}, multiplied by the relevant yields. The results are shown in the last column of Table 3. It should be emphasized that the procedure adopted for the optimization was rather arbitrary and, therefore, the values shown in Table 3 should only be considered as indicative. For example, since no sign of an endothermic transition associated with a PA phase was ever found in the DSC traces of the R^2_{sol} fractions, it was concluded that these fractions consisted of pure CP, even if the presence of small amounts of PA, in the form of short branches of CP-*g*-PA copolymers could not be excluded completely. Conversely, since in the DSC trace of the R^1_{sol} fraction of the l-HDPE-*g*-MA/PA blend a weak first order transition associated with the CP phase was clearly visible, a small concentration of CP was assumed to be present also in the analogous fractions of the other blends and its magnitude was calculated by difference. Despite of this approximation, we believe that the values shown in the last column of Table 3 provide a reliable estimation of the composition of the fractions. Although small amounts of the CP-*g*-PA copolymers may also be present in the other fractions, they are certainly the main components of the R^2_{insol} fractions. The DSC traces in Fig. 5 and the calorimetric data in Table 3 show that the fusion/crystallization temperatures of the two components of these biphasic fractions are much lower than those of the corresponding pure materials and confirm the presence of strong interactions between the phases.

The yields of the R^2_{insol} fractions vary with the type of CP (cf. Table 3). For the l-HDPE-*g*-MA/PA blend, the amount of this fraction is about twice that found for the blends with the two other CPs. Moreover, the very small quantity of R^2_{sol}

a) reaction with the amine end groups of PA:

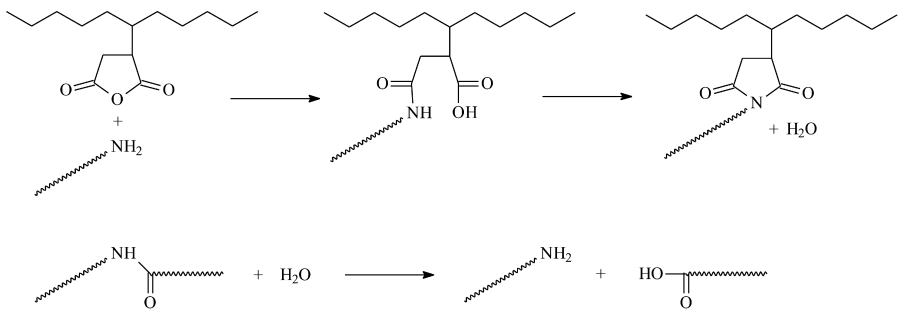

b) reaction with the in-chain amide groups of PA:

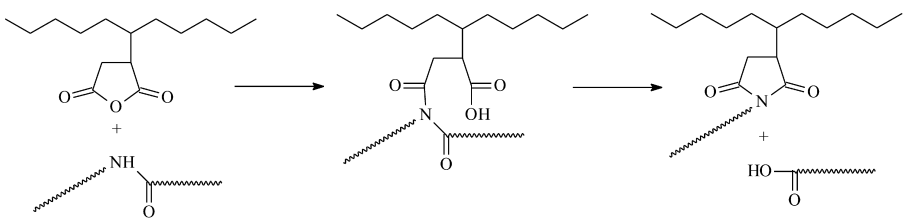

Scheme 1.

material (3.0 wt%) found for the same blend indicates that, contrary to the other CPs, l-HDPE-*g*-MA was almost completely consumed to form a graft copolymer with PA. These findings indicate that l-HDPE-*g*-MA is much more efficient than the other CPs for the production of a CP-*g*-PA copolymer. The composition of the copolymers, as indicated by the values given in the last column of Table 3 for the R^2_{insol} fractions, also varies with the type of CP. In fact, the PA/CP ratio is about 2 for LD08-*g*-MA and l-HDPE-*g*-MA, and exceeds 6 for h-HDPE-*g*-MA.

From the results of the characterization of the binary CP/PA blends we concluded that the reactivity toward PA of the CPs investigated in this work increases in the order h-HDPE-*g*-MA < LD08-*g*-MA < l-HDPE-*g*-MA. The different behavior of the two HDPE CPs can probably be explained by the lower molar mass and/or by the expectedly more uniform distribution of the reactive succinic groups of the commercial CP sample (l-HDPE-*g*-MA).

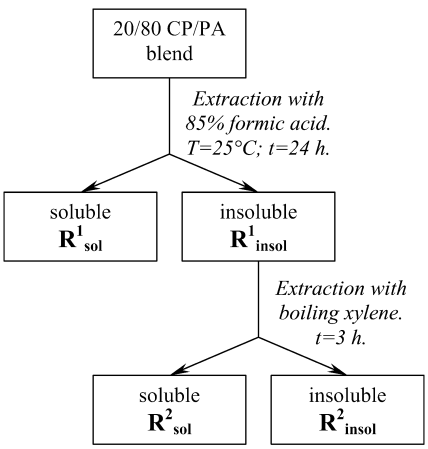

Scheme 2.

3.2. Ternary LDPE/PA/CP blends

The DSC characterization of the ternary LD08/PA/CP and LD03/PA/CP blends demonstrated that, as already found for the blends containing the EAA copolymers [21], the thermal behavior of the LDPE matrix is practically unaffected by the presence of the CPs, whereas the temperatures and the enthalpies of the melting/crystallization transitions of PA are slightly reduced. Moreover, a

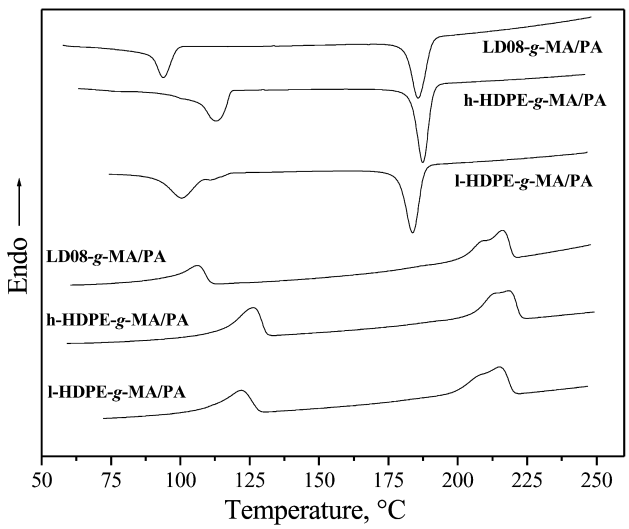

Fig. 5. DSC traces of the R^2_{insol} residues of the 20/80 CP/PA blends.

Table 3
Yields, thermal characteristics and composition of the fractions of the 20/80 CP/PA blends

Blends and fractions	Yield (wt%)	CP phase				PA phase				Composition CP/PA (wt/wt)
		T_c (°C)	ΔH_c[a] (J/g)	T_m (°C)	ΔH_m[a] (J/g)	T_c (°C)	ΔH_c[a] (J/g)	T_m (°C)	ΔH_m[a] (J/g)	LD08-*g*-MA/PA
		95.7	72.3	108.4	55.6	185.2	53.9	218.5	56.0	20/80
R^1_{sol}	72.5	–	–	–	–	186.2	52.3	218.5	55.2	6/94
R^1_{insol}	27.5	95.6	36.4	109.0	37.2	184.7	28.4	214.8	25.1	57/43
R^2_{insol}	17.5	92.8	21.3	106.6	22.6	185.0	44.7	217.0	44.7	33/67
R^2_{sol}	10.0	97.4	63.1	110.3	69.0	–	–	–	–	100/0
h-HDPE-*g*-MA/PA		115.1	156.7	128.5	148.8	186.8	54.8	215.5	53.1	20/80
R^1_{sol}	67.1	–	–	–	–	186.5	58.5	219.0	60.6	1/99
R^1_{insol}	32.9	116.0	92.4	130.2	90.7	189.2	29.7	219.0	29.3	62/38
R^2_{insol}	14.1	112.9	35.1	126.1	37.6	187.4	44.3	218.1	45.6	13/87
R^2_{sol}	18.8	116.1	143.8	129.8	147.6	–	–	–	–	100/0
l-HDPE-*g*-MA/PA		102.7	138.4	124.4	136.7	185.1	52.2	219.6	53.9	20/80
R^1_{sol}	68.5	102.1	19.2	125.7	18.0	187.4	48.1	220.2	49.7	10/90
R^1_{insol}	31.5	101.3	62.3	125.8	55.2	184.4	28.8	218.7	29.7	42/58
R^2_{insol}	28.5	100.4	38.5	121.9	36.4	183.8	44.3	214.9	43.1	37/63
R^2_{sol}	3.0	114.8	163.4	130.2	176.8	–	–	–	–	100/0

[a] Values normalized to the overall amount of the fraction.

change of the content of succinic anhydride groups in the 0.3–3.0 wt% range was found to have negligible effect on the thermal properties of the blends. Representative examples of the DSC traces illustrating this behavior are shown in Fig. 6.

The SEM micrographs of the fracture surfaces of the 75/25 LD08/PA and LD03/PA blends containing different amounts of LD08-*g*-MA (3.0 wt%) are shown in Figs. 7 and 8, and some of the corresponding particle size distributions curves are shown in Fig. 9. The inset in Fig. 9a provides an example of the procedure employed for drawing the frequency curves. The latter show quite clearly that the average dimension of the dispersed PA droplets decreases

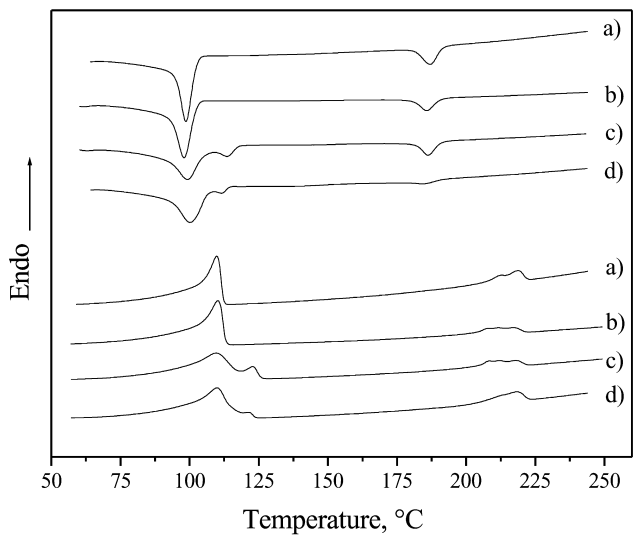

Fig. 6. DSC traces of the 75/25/*x* LD08/PA/CP blends. (a) $x = 0$; (b) CP = LD08-*g*-MA (3.0 wt%), $x = 8$ phr; (c) CP = h-HDPE-*g*-MA, $x = 8$ phr; (d) CP = l-HDPE-*g*-MA, $x = 8$ phr.

appreciably with an increase of the CP concentration, and that the size distribution becomes considerably narrower.

The emulsification curves found for the LD03/PA/LD08-*g*-MA, LD08/PA/LD08-*g*-MA and LD08/PA/l-HDPE-*g*-MA blends are shown in Fig. 10. In the same Fig. are also plotted, as a function of the CP content, the values of the final torque recorded while preparing the blends. The data indicate that the addition of increasing amounts of the CPs causes a progressive reduction of the droplet size and, concurrently, an increase of the melt viscosity. This corroborates the hypothesis that the CP acts as a modifier of the interface properties of these blends.

The addition of only 3 phr LD08-*g*-MA in the LD03/PA blend results in the formation of spherical particles of PA, with an average diameter of 1.25 μm (Fig. 10). Although the measure of the particle size of the PA was not reliable for the uncompatibilized blend (cf. Fig. 8a), we can estimate that the size reduction caused by the addition of 3 phr CP is about twenty-fold. The emulsification curve of this blend still shows a decreasing trend in the LD08-*g*-MA content range investigated, suggesting that no saturation of the interface is obtained, even with 8 phr.

The emulsification curves obtained for the 75/25 LD08/PA blend differ considerably from each other, depending on the nature of the CP. With l-HDPE-*g*-MA, the droplet size decreases steeply in the CP content range up to 2 phr, and much more slowly thereafter. The behavior of this CP closely resembles that of the EAA copolymers [21]: in that case, however, the limiting droplet size was slightly higher (about 0.6 μm) and the saturation concentration of the CP was smaller (about 1 phr). The difference in the saturation concentration is probably due to a higher concentration of carboxyl groups of the EAA copolymers. The CPs described in this work, however, are evidently

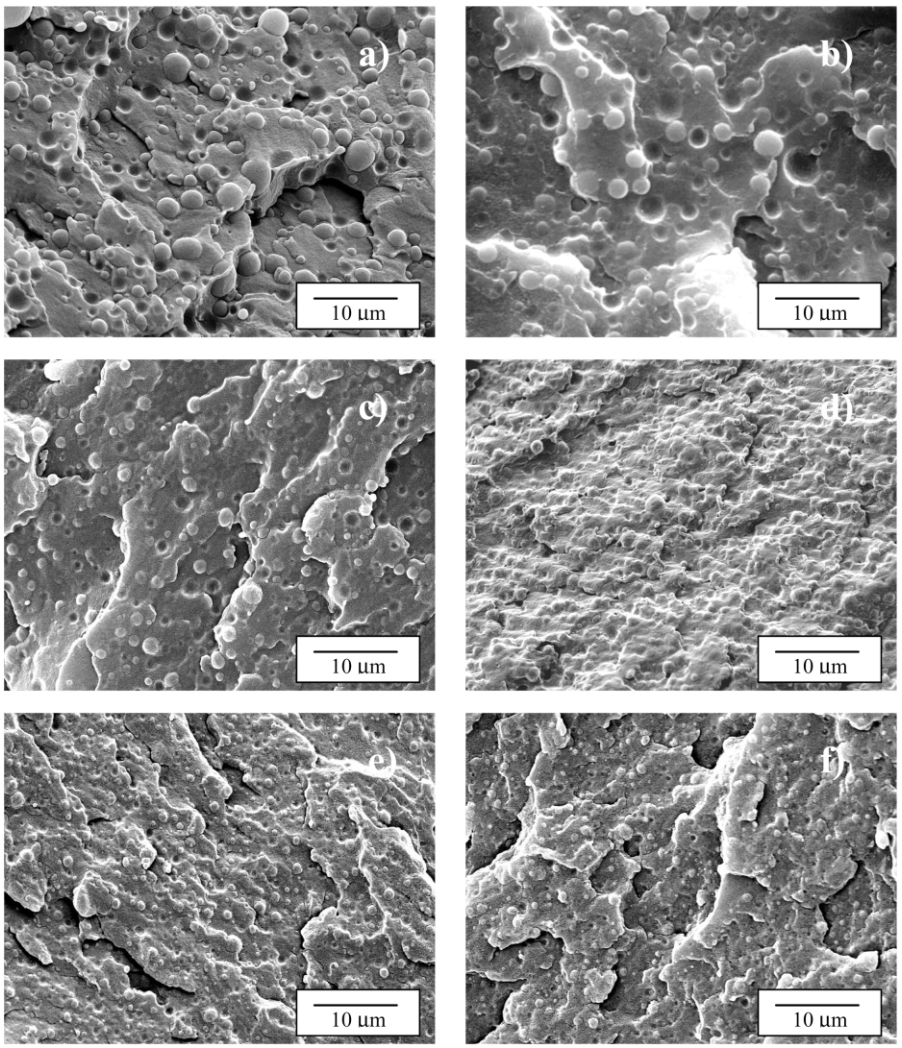

Fig. 7. SEM micrographs of the 75/25/x LD08/PA/LD08-g-MA (3.0 wt%) blends. (a) $x = 0$ phr; (b) $x = 1.5$ phr; (c) $x = 3$ phr; (d) $x = 5$ phr; (e) $x = 8$ phr; (f) $x = 10$ phr.

more effective in enhancing the dispersion of the PA droplets, presumably because of the higher reactivity of the anhydride groups toward PA.

The behavior of the LD08/PA/LD08-g-MA blend shown in Fig. 10 clearly indicates that the effectiveness of LD08-g-MA, as a CP for the LD08/PA blend, is considerably lower than that of l-HDPE-g-MA. Indeed, the droplet size recorded with the former CP is much larger in the whole range of concentration investigated. Surprisingly, although the concentration of grafted MA in the LD08-g-MA (3 wt%) is three times that in the l-HDPE-g-MA copolymer, no saturation of the interface is achieved until the content of LD08-g-MA exceeds 10 phr. A reasonable explanation is offered by examining the results of the DSC and SEM study. These data show that LD08-g-MA is miscible with LD08, whereas biphasic systems are formed by blending LD08 with the MA-functionalized HDPEs. Therefore, during the preparation of the ternary blends, the HDPE CPs can easily migrate to the interface between the LD08 and PA phases, where the grafting reaction occurs, whereas LD08-g-MA tends to dissolve in the LD08 matrix and the reaction with PA is retarded.

An emulsification curve for the 75/25 LD08/PA blend compatibilized with h-HDPE-g-MA was not obtained because this CP proved particularly ineffective: even a concentration of 8 phr failed to lower the PA droplet size below 1 μm. Direct evidence of the different efficiencies of the three types of CP used in this work is provided by the micrographs shown in Fig. 11, taken on 75/25 LD08/PA blends compatibilized with 8 phr of LD08-g-MA, h-HDPE-g-MA and l-HDPE-g-MA. Although the interfacial adhesion is fairly good in all three blends, the PA droplets dispersion increases in the order h-HDPE-g-MA $<$ LD08-g-MA $<$ l-HDPE-g-MA. The inefficiency of h-HDPE-g-MA relative to l-HDPE-g-MA is obviously an effect of the higher molar mass and/or the less uniform distribution of the reactive succinic groups in h-HDPE-g-MA.

It was also of interest to investigate the dependence of the minor phase droplet size on the MA grafting degree of the CPs. This study was carried out on the 75/25 LD08/PA

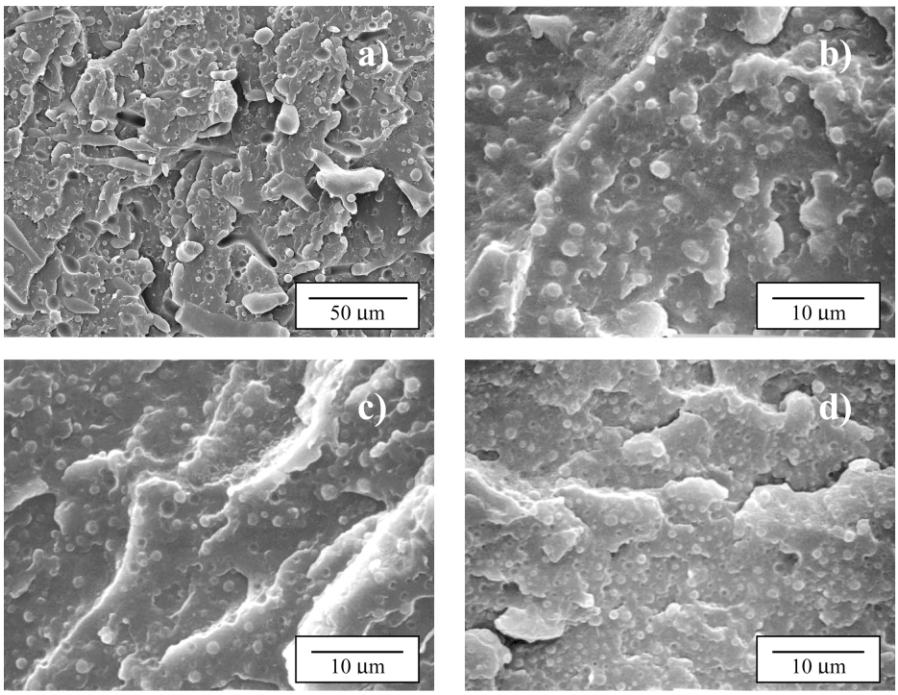

Fig. 8. SEM micrographs of the 75/25/x LD03/PA/LD08-g-MA (3.0 wt%) blends. (a) $x = 0$ phr; (b) $x = 3$ phr; (c) $x = 5$ phr; (d) $x = 8$ phr.

blends compatibilized with 8 phr of LD08-g-MA. The results, shown in Fig. 12, indicate that a strong enhancement of dispersion of the PA droplets is found by using a CP with only 0.3 wt% MA, and that no further improvement is obtained by increasing the grafting degree beyond 0.8 wt%. In this case too, the effect is paralleled by an increase of the melt viscosity, as indicated by the final torque measured at the end of the blending process. These results are in good agreement with those of Borggreve and Gaymans [33], who studied the behavior of blends of PA with a MA-grafted EPDM rubber. These authors found that the concentration of the coupling agent, within the range 0.13–0.89%, had negligible effects on either the dispersion process or the impact properties of the blends. The results described in this paper, however, are at variance with those of a previous study [21], in which EAA copolymers were used as compatibilizer precursors. In that case, the effectiveness increased with an increase of the acrylic acid content from 6.2 to 11.0 wt%. This discrepancy is probably due to a difference in the CPs microstructure. Since the EAA copolymers were characterized by random distribution of the functional acrylic acid moieties along the PE chains, it is not surprising that an increase of their degree of functionalization enhances the reactivity toward PA. The CPs studied in this work, contain succinic anhydride groups that have been incorporated in the PE chains by grafting. Although it is known [34,35] that the MA grafting takes place predominantly by incorporation of single succinic groups, due to poor homopolymerization capability of MA, the anhydride groups are apparently grafted onto the polyolefin chain in close proximity to each other [36]. Therefore, the CPs used in this work may actually consist of blends of ungrafted PE chains with PE macromolecules containing clusters of succinic anhydride groups whose reactivity may be hindered by steric factors.

4. Conclusions

The MA-grafted polyolefins are known to be efficient CPs for blends of condensation polymers (especially polyamides) with polyolefins. This work demonstrates that the effectiveness of different PE-g-MA copolymers for the reactive compatibilization of LDPE/PA blends is greatly influenced by the microstructure and the MFI of the PE substrate. In particular, the CPs consisting of LDPE-g-MA copolymers were inefficient because they are miscible with the LDPE component and hardly available at the blend interface, where the reactions with PA are expected to occur. The effectiveness of these CPs was found to be almost independent of the concentration of the succinic reactive groups. Conversely, the CPs with HDPE backbones are not miscible with LDPE and can easily migrate to the LDPEPA interface, where reactive compatibilization takes place. The best CP performance is observed when the molar mass of the HDPE substrate is low, and the distribution of the succinic groups along the chains is rather uniform. Among the CPs investigated in this work, a commercial sample of HDPE-g-MA of relatively high MFI was found to be most effective. The efficiency of MA-grafted CPs compares favorably with that of the EAA copolymers studied in a previous work.

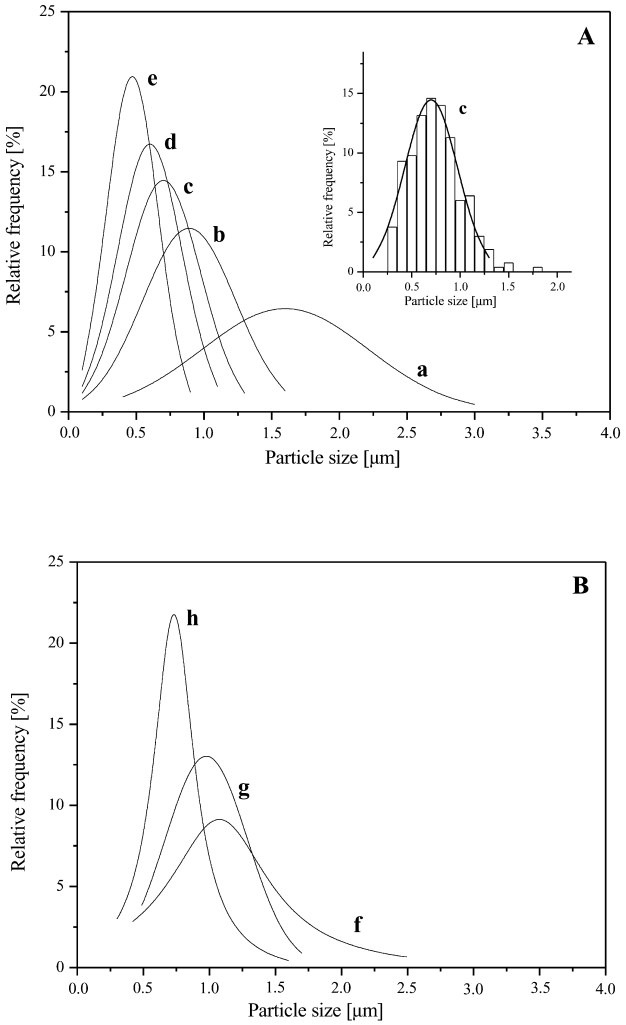

Fig. 9. Particle size distribution for the 75/25/*x* LD08/PA/LD08-*g*-MA (3.0 wt%) (A), and LD03/PA/LD08-*g*-MA (3.0 wt%) (B) blends. (a) $x = 0$ phr; (b) $x = 3$ phr; (c) $x = 5$ phr; (d) $x = 8$ phr; (e) $x = 10$ phr; (f) $x = 3$ phr; (g) $x = 5$ phr; (h) $x = 8$ phr. Inset: construction procedure for curve (c).

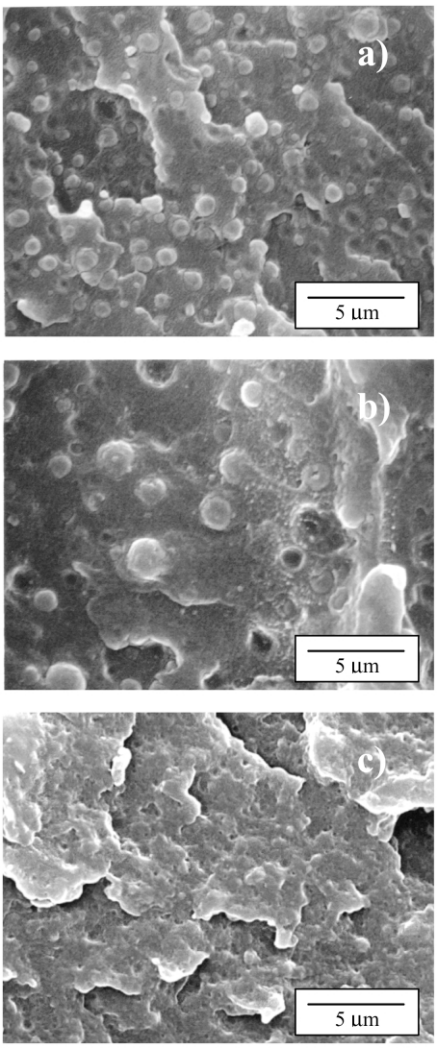

Fig. 11. SEM micrographs of the 75/25/8 LD08/PA/LD08-*g*-MA (0.8 wt%) (a), LD08/PA/h-HDPE-*g*-MA (b), and LD08/PA/l-HDPE-*g*-MA (c) blends.

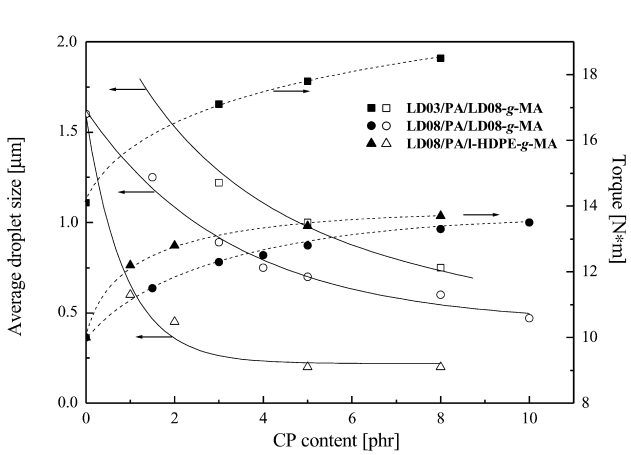

Fig. 10. Average droplet size and final torque versus CP content for some 75/25/*x* LDPE/PA/CP blends.

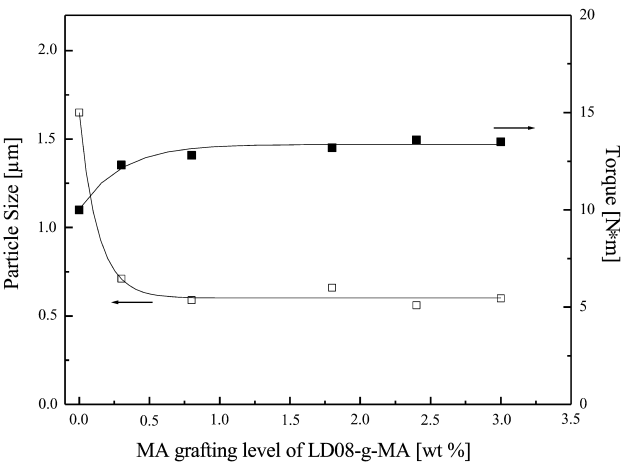

Fig. 12. Average droplet size and final torque of the 75/25/8 LD08/PA/LD08-*g*-MA blends, as a function of the MA content of the CP.

Acknowledgements

This work was financially supported by the Italian Ministry of University and Scientific and Technological Research (MURST), contract no MM09244737. Thanks are due to Polimeri Europa, Snia Tecnopolimeri and Uniroyal for providing samples of the polymers used in this work. C.J. is grateful to Prof. Elena Galoppini of Rutgers University-Newark. Thanks are due to Prof. L. Minkova of the Institute of Polymers, Bulgarian Academy of Sciences, for many useful discussions, and to Mr P. Narducci, University of Pisa, who made the electron microscopic analyses.

References

[1] Chen CC, Fontan E, Min K, White JL. Polym Engng Sci 1988;28(21): 69–80.
[2] Willis JM, Favis BD. Polym Engng Sci 1988;28(21):1416–26.
[3] Serpe G, Jarrin J, Dawans F. Polym Engng Sci 1990;30(9):553–65.
[4] Kim BK, Park SY, Park SJ. Eur Polym J 1991;27:349–54.
[5] Padwa AR. Polym Engng Sci 1992;32(22):1703–10.
[6] Yeh JT, Fan-Chiang CC, Cho MF. Polym Bull 1995;35:371–8.
[7] Hu GH, Sun YJ, Lambla M. Polym Engng Sci 1996;36(5):676–84.
[8] Yeh JT, Fan-Chiang CC, Yang SS. J Appl Polym Sci 1997;64: 1531–40.
[9] Sánchez-Valdes S, Yañez-Flores I, Ramos de Valle LF, Rodriguez-Fernandez OS, Orona-Villarreal F, Lopez-Quintanilla M. Polym Engng Sci 1998;38(1):127–33.
[10] Jurkowski B, Kelar K, Ciesielska D. J Appl Polym Sci 1998;69: 719–27.
[11] Lee SY, Kim SC. J Appl Polym Sci 1998;67:2001–14.
[12] Gadekar R, Kulkarni A, Jog JP. J Appl Polym Sci 1998;69:161–8.
[13] Chen CC, Fontan E, Min K, White JL. Polym Engng Sci 1998;28(2): 69–80.
[14] Lazzeri A, Malanima M, Pracella M. J Appl Polym Sci 1999;74: 3455–68.
[15] Kudva RA, Keskkula H, Paul DR. Polymer 1999;40:6003–21.
[16] Yao Z, Yin Z, Sun G, Liu C, Tong J, Ren L, Yin J. J Appl Polym Sci 2000;75:232–8.
[17] Kelar K, Jurkowski B. Polymer 2000;41:1055–62.
[18] Pan L, Chiba T, Inoue T. Polymer 2001;42:8825–31.
[19] Pan L, Inoue T, Hayami H, Nishikawa S. Polymer 2002;43:337–43.
[20] Jurkowski B, Olkhov YA, Kelar K, Olkhova OM. Eur Polym J 2002; 38:1229–36.
[21] Filippi S, Chiono V, Polacco G, Paci M, Minkova L, Magagnini P. Macromol Chem Phys 2002;203:1512–25.
[22] Samay G, Nagy T, White JL. J Appl Polym Sci 1995;56:1423–33.
[23] Clark DC, Baker WE, Whitney RA. J Appl Polym Sci 2001;79: 96–107.
[24] Bettini SHP, Agnelli JAM. Polym Test 2000;19:3–15.
[25] Gaylord NG, Mehta R, Mohan DR, Kumar V. J Appl Polym Sci 1992; 44:1941–9.
[26] Gaylord NG, Mehta R. J Polym Sci Part A: Polym Chem 1988;26: 1189–98.
[27] Molau GE. Kolloid Z Z Polym 1970;238:493–8.
[28] Illing G. Angew Makromol Chem 1981;95:83–108.
[29] Pötschke P, Wallheinke K, Janke A, Bellmann C. J Macromol Sci Phys 1999;B38:527–39.
[30] Maréchal P, Coppens G, Legras R, Dekoninck JM. J Polym Sci Part A: Polym Chem 1995;33:757–66.
[31] Raval H, Devi S, Singh YP, Mehta MH. Polymer 1991;32:493–500.
[32] Sathe SN, Devi S, Srinivasa Rao GS, Rao KV. J Appl Polym Sci 1996; 61:97–107.
[33] Borggreve RJM, Gaymans RJ. Polymer 1989;30:63–70.
[34] Heinen W, Rosenmoller CH, Wenzel CB, de Groot HJM, Lugtenburg J. Macromolecules 1996;29:1151–7.
[35] Russell KE, Kelusky EC. J Polym Sci Part A: Polym Chem 1988;26: 2273–80.
[36] Ranganathan S, Baker WE, Russell KE, Whitney RA. J Polym Sci Part A: Polym Chem 1999;37:3817–25.